Revista Brasileira de Recursos Hídricos
Brazilian Journal of Water Resources
Versão On-line ISSN 2318-0331
RBRH, Porto Alegre, v. 26, e31, 2021
Scientific/Technical Article

https://doi.org/10.1590/2318-0331.262120210087

Statistical analysis of hydrochemistry and isotopic characterization of groundwater from the Parecis Basin

Análise estatística da hidroquimica e caracterização isotópica das águas subterrâneas da Bacia dos Parecis

Marcia Regina Stradioto[1], **Elias Hideo Teramoto**[1] & **Hung Kiang Chang**[1]

[1]Universidade Estadual Paulista, Rio Claro, SP, Brasil
E-mails: marcia.stradioto@unesp.br (MRS), elias.hideo-teramoto@unesp.br (EHT), chang.hung-kiang@unesp.br (HKC)

Received: June 17, 2021 - Revised: August 25, 2021- Accepted: August 27, 2021

ABSTRACT

Knowledge of mechanism controlling the hydrochemistry of groundwater are crucial requirement to understand the hydrochemical evolution and evaluate the water quality of subsurficial water resources. Thus, to understand the process governing the hydrochemistry variability and flow dynamics of the Parecis and Ronuro Aquifers, the use of statistical analysis and isotopic characterization were combined. In the correlation matrix it was found that the highest correlation coefficient was observed for HCO_3^-, Ca^{2+}, Mg^{2+}, Sr^{2+}, SO_4^{2-}, and F^-, which suggested that these parameters are derived from the same source, most likely from rock–water interactions. Additionally, we noticed moderate to high correlation among NO_3^-, Cl^-, Na^+, K^+, and Ba^{2+}, which collectively are indicative of domestic sewage contamination. Finally, a principal component analysis (PCA) identified that the most variance in hydrochemistry from the evaluated samples was controlled by HCO_3^-, Ca^{2+} and Mg^{2+}, which is associated with rock–water interaction. Regarding the ^{18}O and ^{2}H isotope values, it could be observed that the aquifer recharges were of meteoric origin and that the Ronuro Aquifer samples were more enriched than the PAS samples. This work reinforces the capability of multivariate statistics to discern the main process that controls the variability of groundwater hydrochemistry.

Keywords: Hydrochemistry; Parecis aquifer; Ronuro aquifer; Multivariate statistics; Stable isotopes.

RESUMO

O conhecimento dos mecanismos que controlam a hidroquímica das águas subterrâneas é um requisito fundamental para compreender a evolução hidroquímica e avaliar a qualidade da água dos recursos hídricos subterrâneos. Por consequência, para compreender o processo que governa a variabilidade da hidroquímica e dinâmica de escoamento dos aquíferos Parecis e Ronuro, foi empregado uma abordagem combinando o uso de análises estatísticas e caracterização isotópica. A matriz de correlação permitiu verificar que os maiores coeficientes de correlação foram observados entre HCO_3^-, $Ca^{2+,}$ Mg^{2+} - $Sr^{2+,}$ $SO_4^{2-.}$ e F^-, sugerindo que esses parâmetros são derivados da mesma fonte, provavelmente a interação rocha/água. Adicionalmente, também observamos correlação moderada a alta entre NO_3^-, Cl^-, Na^+, K^+ e Ba^{2+}, que coletivamente são indicativos da contaminação por efluente doméstico. Complementarmente, a Análise de Componentes Principais permitiu identificar que grande parte da variância da histoquímica das amostras avaliadas é controlada por HCO_3^-, Ca^{2+} e Mg^{2+} associados à interação rocha-água. Quanto aos valores dos isótopos ^{18}O e ^{2}H, foi possível notar que as recargas do aquífero são de origem meteórica e que as amostras do Aquífero Ronuro são mais enriquecidas que as amostras SAP. Os resultados alcançados reforçam a capacidade das técnicas de análise estatística multivarida para discernir o processo principal que controla a variabilidade da hidroquímica da água subterrânea.

Palavras-chave: Hidroquímica; Aquífero Parecis; Aquífero Ronuro; Estatística multivariada; Isótopos estáveis.

INTRODUCTION

Groundwater constitutes the main source of water for drinking, irrigation, and industrial purposes in numerous regions around the world, especially in those regions where the surface water is scarce (e.g., Kemper, 2004; Robins & Fergusson, 2014). The scarcity of groundwater is a problem that is intrinsically attributed to both quantity and quality factors. While the quantity factors include the volume of groundwater stored in the aquifers (Kemper, 2004), the quality is influenced by natural and anthropogenic processes, which is a key factor that may impact human health or end-use purposes (Singh et al., 2006).

The mechanisms controlling the hydrochemical characteristics of groundwater cover a large variety of processes. Among them, mixing with brackish water (e.g., El Alfy et al., 2018), evaporation (e.g., Maurya et al., 2019), rock-water interaction (e.g., Kumar et al., 2020; Stradioto et al., 2020a), and anthropogenic actions (e.g., Stradioto et al., 2020b) are especially relevant. Due to the complexity and overlap of the processes controlling the hydrochemistry of groundwater, different approaches have been proposed to understand the hydrochemistry variability of groundwater, such as multivariate statistics and geochemical simulation.

Owing to the abundance of the evaluated parameters in hydrochemistry characterization, the use of multivariate statistics comprises a convenient and effective way to interpret the analytical data and identify the hydrochemical facies, which, in turn, allows for the identification of either the geochemical process controlling the water quality or the anthropogenic contamination (e.g., Mouser et al., 2005; Manoj et al., 2013; Ahada & Suthar, 2017; Said et al., 2020). Moreover, multivariate statistics is efficient for identifying and characterizing subtle hydrochemical anomalies (O'Shea & Jankowski, 2006). Complementing the multivariate statistics, geochemical simulations are a powerful tool for assessing the process impacting the hydrochemistry and performing mass balance (e.g., Yang et al., 2018; Barzegar et al., 2018; Christofi et al., 2020; Stradioto et al., 2020a). Some research works have demonstrated that the combined use of multivariate statistics and geochemical simulations can be a beneficial approach for identifying and examining the main process controlling the water quality (e.g., Helstrup et al., 2007; Marghade et al., 2021; Teramoto et al., 2019; Liu et al., 2020).

Regarding hydrochemical characteristics, the Parecis Aquifer System (PAS) represents one of the least studied aquifers in Brazil. Covering an area of 88,147 km^2, PAS outcrops in the west of the state of Mato Grosso and the east of Rondônia, with an average saturated thickness of 150 m. This system is formed by sandstones with intercalations of conglomerate levels and pelitic lenses of Cretaceous age; its estimated exploitable reserve is 464.8 m^3/s (Agência Nacional de Águas, 2007), and it is generally explored in free conditions. Due to its high productivity—an average flow of 146.9 m^3/h and an average specific capacity of 8.83 m^3/h/m—this aquifer is widely used as source of water supply as well as agricultural and industrial uses (Agência Nacional de Águas, 2007). However, the Parecis Aquifer System presents risks of contamination, mainly in its outcrop area, related to agriculture and the recent process of urbanization, lacking a sewage collection system (Serviço Geológico do Brasil, 2012a). Despite its importance and high vulnerability, the study of the key process controlling the water quality of the Parecis Aquifer System, especially in relation to contamination, is poor. Thus, to fill this gap, in this work, we have used a combination approach of statistical analysis of hydrochemistry and isotopic analysis to trace the mechanisms governing the hydrochemistry of the continental aquifers that are impacted by anthropogenic actions.

GEOLOGICAL AND HYDROGEOLOGICAL SETTING

Regional geology

Recognized as one of the largest intracratonic basins in Brazil and formed by an elongated structure in the general direction W–E, the Parecis Basin occupies an area of approximately 500,000 km^2 in the states of Rondônia and Mato Grosso, with its largest dimension being 1,250 km (Figure 1). It is divided from west to east into three tectono-sedimentary domains (sub-basins): sub-basin of Rondônia, in the extreme west, is a tectonic depression; sub-basin of Juruena, in the central region, is a low gravimetric, and the upper Xingu sub-basin, in the far east, is a synéclise-type interior basin (Figure 2). The Parecis Basin has about 6,000 m of Paleozoic, Mesozoic, and Cenozoic sediments and includes Cretaceous volcanic rocks (spills and dikes); its sediments are essentially siliciclastic (Siqueira, 1989; Bahia, 2007).

The Parecis Basin is divided into nine lithostratigraphic units (Figure 1), deposited between the Ordovician and the Cenozoic periods (Bahia et al., 2006). The Amazonian Craton is the foundation of the Parecis Basin, covering rocks of high and low metamorphism, metasedimentary rocks, and intrusive rocks. The first ones, to the west of the basin, are the granulites of the Jamarí Complex in the state of Rondônia and the gneisses, migmatites, and granitoids of the Xingu Complex, to the north and south of the basin, of Archaean and Mesoproterozoic age in the states of Mato Grosso and Goiás. Metasedimentary rocks emerge in the southeast part of the basin in the states of Mato Grosso and Goiás. The basic and ultrabasic intrusive rocks are related to the Mesoproterozoic era (Bahia et al., 2006).

The filling of the Parecis Basin began in the Paleozoic age with the deposition of conglomerates, sandstones, siltstones, and shales, in the same order towards the top, with a few contributions from carbonate and glacial sediments. The sedimentary package consists of, from base to top, the Cacoal, Pimenta Bueno, and Fazenda da Casa Branca formations (west of the basin) and of the Furnas and Ponta Grossa formations (east of the basin) (Bahia, 2007). In the Lower Paleozoic, the Amazonian region was affected by an extensional event that implemented a system of intracontinental rifts, which were filled at least in part by Cacoal formations during the Ordovician age. The Cacoal, Furnas, Ponta Grossa, Pimenta Bueno, Casa Branca Farm, Rio Ávila and the Parecis Group deposited on this rift system (Bahia, 2007).

In the Mesozoic (Juro-Cretaceous) era, another extensional event that impacted the Amazon region was related to the separation between South America and Africa, when depressions were filled by sedimentary and volcanic rocks. In this basin, this event corresponds to the basaltic spills of the Anari and Tapirapuã formations that occurred around 198 Ma, which were covered

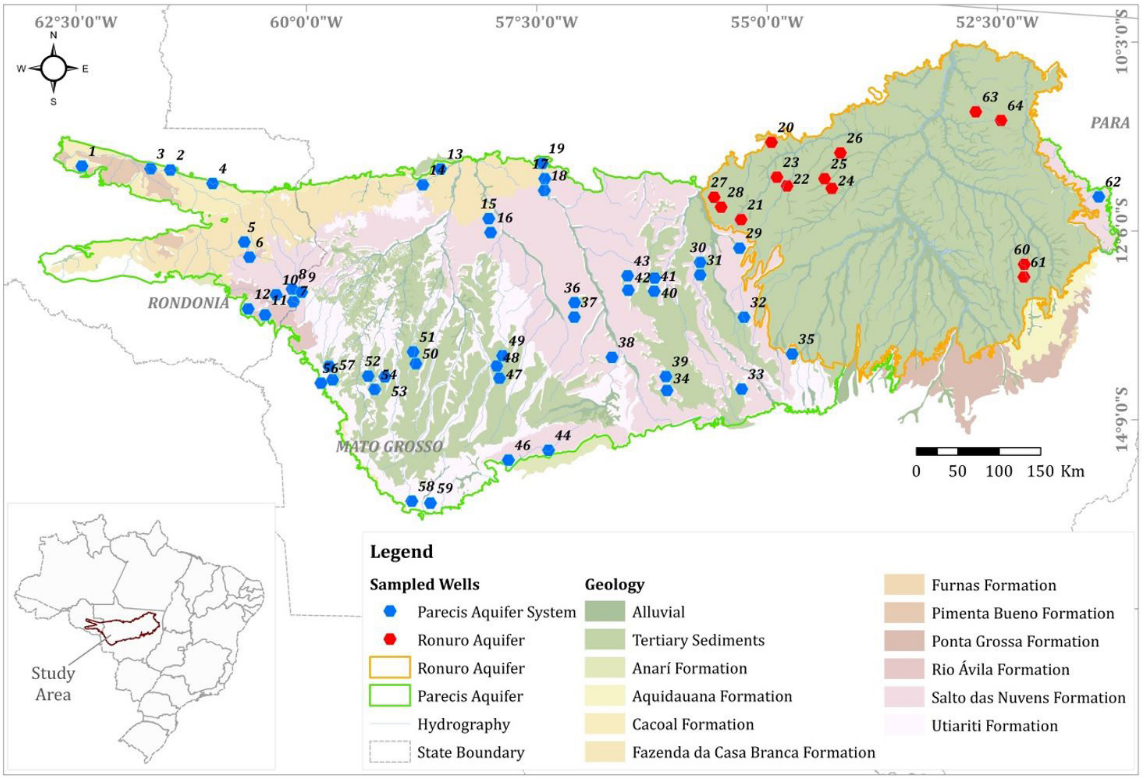

Figure 1. Geology and location of the study area with the distribution of sampled wells. Source: geology: Bahia et al. (2007); aquifer contour: Agência Nacional de Águas (2013). WNW = North/Nortwest; ESE = East/Southeast.

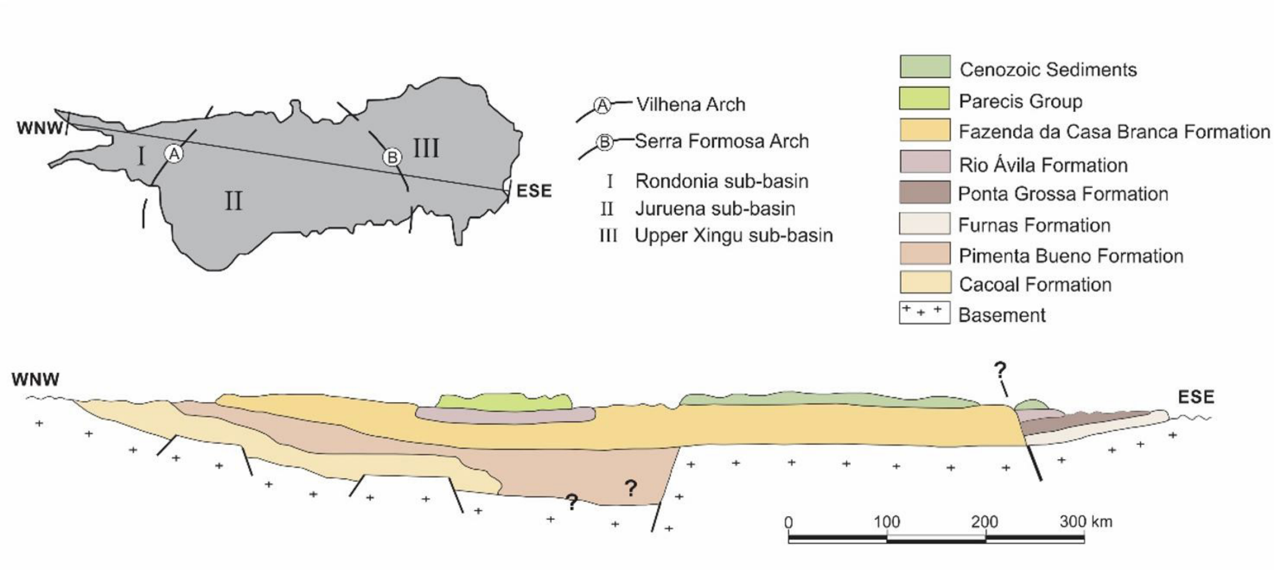

Figure 2. Geological section of the Parecis Basin. Source: Bahia (2007).

by the Rio Ávila Formation. The Parecis Group was deposited in the Cretaceous. The aforementioned lithostratigraphic units form five depositional sequences, namely, Ordovician, Devonian, Carboniferous-Permian, Juro-Cretaceous, and Cretaceous, separated by regional unconformity, indicating deposition in a synéclise basin of the continental interior (Bahia et al., 2007).

Hydrogeological setting

The PAS is formed by sandstones with intercalations of conglomerate levels and pelitic lenses of Cretaceous age, with an estimated exploitable reserve of 464.8 m^3/s, generally in free conditions; however, it can present conditions of semi-definition by lateritic coverings and clayey. It has excellent productivity, with an average flow of 146.9 m^3/h and an average specific capacity of 8.83 $m^3/h/m$ (Agência Nacional de Águas, 2007).

In the state of Rondônia, PAS has an area of approximately 20,000 km^2, bordered by the Pimenta Bueno and Colorado grubs and the Colorado Complex (west), the Rio Pardo intrusive suite (north), and the Colorado Complex (south). However, to the east, it exceeds the limit of the state of Rondônia and enters the state of Mato Grosso. This system consists of the Utiariti, Fazenda da Casa Branca, and Rio Ávila Formations and represents the largest flows and depths of the state of Rondônia. Alluvial sediments and coverings, although associated with the rocks of this system, have a small hydrogeological vocation (Serviço Geológico do Brasil, 2012a). Groundwater from PAS is of good chemical quality. Morais (1998) from seven samples classified the waters of the Parecis Aquifer System as sodium chloride type. The electrical conductivity and the dry residue proved to be extremely low, with an average of 15.4 μS/cm and 24 mg/L, respectively (Serviço Geológico do Brasil, 2012a).

In the PAS, two aquiferous subtypes were identified that were determined as free subsystem and confined subsystem. The basis of this subdivision is the relation among hydrodynamic parameters and the characteristics of the lithological profiles of the inventoried tubular wells (Silva, 2013).

The Ronuro Aquifer has a stratigraphic position that guarantees the important recharge function of the underlying aquifers and also that the hydrological system of the upper Xingu is well fed. Many tubular wells currently explore the groundwater flowing through this aquifer, with depths ranging between 18 and 140 m and totaling more than 6000 m drilled in the aquifer. The exploitation flows range from 1 to 105 m^3/h and an average of 10.42 m^3/h, with a specific regional flow of around 1.5 $m^3/h/m$. The highest flows are concentrated in the Sinop region, while the lowest are concentrated in the regions of the municipalities of Querência and Cláudia. Static levels vary between 1 and 32 m, with an average of around 13 m in depth (Serviço Geológico do Brasil, 2012b).

According to the information from SIAGAS, more than 270 tubular wells take advantage of the groundwater circulating in the Parecis Group and Ronuro Formation. The Salto das Nuvens Formation has the highest number of registered wells (46.5%), followed by the Ronuro Aquifer (44.7%). Most of the wells are for domestic supply since 47.6% are privately owned, including agricultural cooperatives and traders.

MATERIAL AND METHODS

Hydrochemistry dataset

For hydrochemical and isotopic analyzes, 63 samples of groundwater distributed in the Parecis Basin in the states of Mato Grosso and Rondônia were collected. Of these samples, 50 explore the Parecis Aquifer, while the remaining 13 explore the Ronuro Aquifer (Figure 1). Prior to collection, the pumps in the wells were switched on for a few minutes to ensure the renewal of stagnant water in the pipeline and the well. The collections were carried out at the well before the treatment processes, such as fluoridation, chlorination, and/or water storage.

During sampling, pH, electrical conductivity, and temperature were measured. Moreover, in the field, the samples were filtered in a Millipore^{MR} set of 0.45 μm. The samples sent for analysis of cations were acidified with concentrated nitric acid (14.4 molar), with two drops for each 50 mL of sample. The closed bottles were kept refrigerated until they were delivered to the IGCE Hydrogeology and Hydrochemistry laboratory and to the Center for Environmental Studies (CEA), UNESP, Rio Claro campus, where the samples were analyzed.

To determine the elements Ca, Fe, Mg, Mn, Sr, Ba, Zn, Pb, Si, Al, Ni, Cr, P, Cu, Co, and Cd, the optical emission spectrometry method was used, with a plasma source of inductive argon (ICP-OES). Alkalinity (HCO_3^- and $CO_3^{2-)}$ was obtained by acid titration; anions (F^-, Cl^-, Br^-, NO_3^-, NO_2^-, SO_4^{2-}, and PO_4^{3-}) and cations (Na^+, K^+, Li^+, and NH_4^+) were determined by ion chromatography (IC). All analyses were developed based on the Standard Methods for the Examination of Water and Wastewater (22nd edition) (American Public Health Association, 2012).

The groundwater sampling for isotopic analyses (^{18}O and ^2H) followed the recommended sampling standards (International Atomic Energy Agency, 2009); these samples were then sent to the Hydrogeology and Hydrogeochemistry Laboratory of the Department of Applied Geology at UNESP, in Rio Claro, SP. For the analysis, the ring-down resonant cavity spectroscopy technique was used, which is based on the absorption of laser radiation in the near-infrared range (0.7 μ to 2.5 μ) by substances in the gaseous state, such as water, carbon dioxide gas, and methane. The instruments used were Liquid Water Isotope Analyzer by Los Gatos Research Inc (models LWIA-24-EP and TLWIA-45-EP). The VSMOW standard (Vienna Standard Mean Ocean Water) was used to determine δ18O and δ2H and the analytical uncertainties were ± 0.4‰ and ± 1.2‰, respectively.

The obtained values of physical-chemical (i.e., electrical conductivity and pH), major cations and anions, as well as the $\delta^{18}O$ and δ^2H are presented in Table 1.

Parametric statistics and matrix of correlation

To summarize the available parameters, we computed their mean, maximum, minimum, and standard deviation values. To evaluate the interrelationship between the physical-chemical (electrical conductivity and pH) and major cations and anions, we build a correlation matrix. We assumed that the parameters possessing high coefficients of correlation (r) have the same origin (e.g., mineral dissolution, sewage contamination, fertilizer). Thus, based on the association identified by the calculated coefficients of correlation, we identified the process governing the concentration of these parameters in groundwater. High values of r indicate the significance of the interrelation between two evaluated parameters. A positive coefficient suggests similarity and harmony between correlated parameters, and a negative coefficient demonstrates that variables are developing in opposite directions.

Table 1. Values of well depth, physical-chemical, major cations and anions, and the $\delta^{18}O$ and $\delta^{2}H$ of the evaluated samples. ND = Not determined.

Sample	Aquifer	Depth	Electrical conductivity	pH	HCO_3^-	Cl^-	SO_4^{2-}	NO_3^-	Ca^{2+}	Mg^{2+}	Na^+	K^+	Si	F^-	Sr^{2+}	Al^{3+}	Ba^{2+}	Fe^{2+}	Pb^{2+}	Zn^{2+}	Mn^{2+}	Cu^{2+}	$\delta^{18}O$	$\delta^{2}H$
		(m)	µS/cm		mg/L																		‰	
1	parecis	80	85.3	6.88	36.7	0.24	8.32	< 0.04	6.41	3.18	4.46	1.51	17.1	0.13	0.04	0.01	0.02	0.07	< 0.005	0.01	0.03	< 0.004	ND	ND
2	parecis	80	171	6.21	21.7	17	3.73	33.2	8.73	1.47	17.5	4.85	13.4	0.10	0.02	0.03	0.31	0.03	< 0.005	< 0.005	0.23	< 0.004	-7.2	-42.9
3	parecis	60	67.8	6.01	7.04	2.27	0.12	21.6	0.23	1.83	4.22	6.52	6.71	0.04	0.01	0.01	0.39	0.04	< 0.005	0.02	0.04	< 0.004	-6.92	-41.5
4	parecis	18	48	6.2	7.24	1.89	3.79	7.27	1.52	1.04	3.69	2.6	5.7	0.09	0.01	0.03	0.04	0.03	< 0.005	0.01	0.01	< 0.004	-6.72	-41
5	parecis	76.5	78.6	6.76	7.3	10.1	2.11	13.4	4.05	0.55	11.4	1.82	3.33	0.03	0.01	0.02	0.08	0.04	0.02	0.10	0.39	0.02	-7.6	-47.1
6	parecis	52	123	4.01	0	5.84	0.07	34.7	0.54	0.31	7.47	1.55	4.43	0.04	< 0.005	0.97	0.05	0.01	0.01	0.01	0.05	0.01	-7.19	-46.5
7	parecis	120	23	6.81	9.22	1.62	0.51	0.38	2.39	0.20	1.62	0.38	3.58	0.01	0.02	0.01	0.01	0.03	< 0.005	0.17	0.03	0.05	-5.63	-40.4
8	parecis	83	26.1	5.92	7.53	1.76	0.22	0.72	1.59	0.21	1.26	0.43	3.52	< 0.01	< 0.005	0.04	0.01	0.04	0.03	0.11	0.01	0.02	-6.5	-44.1
9	parecis	90	10.9	5.19	3.84	0.39	0.22	0.22	0.45	0.05	0.58	1.21	1.58	< 0.01	< 0.005	0.01	< 0.005	0.05	0.02	0.03	0.02	0.01	ND	ND
10	parecis	90	20.6	5.85	7.63	2.26	0.27	0.54	3.16	0.26	1.49	1.44	3.33	0.02	0.01	0.06	0.01	0.02	0.03	0.14	0.02	0.01	-6.09	-42.8
11	parecis	72	382	6.77	99.7	23.7	2.93	45.8	21	17.7	8.55	1.38	21.4	0.17	0.12	0.01	0.21	0.01	0.01	0.01	< 0.001	< 0.004	-6.17	-43.6
12	parecis	35	37.6	5.86	5.92	0.95	0.08	11.8	0.15	0.06	8.03	0.6	2.81	0.02	< 0.005	0.01	0.01	0.04	< 0.005	< 0.005	< 0.001	0.01	-6.77	-47.8
13	parecis	25	113	4.86	1.35	11	3.44	31.2	1.17	2.4	9.98	6.7	5.18	0.05	0.02	0.18	0.57	0.04	0.01	0.03	0.05	0.01	-5.81	-39.7
14	parecis	42	54.2	4.71	0	6.02	0.12	13.8	0.42	0.38	5.97	1.52	4.14	0.02	< 0.005	0.13	0.07	0.01	0.01	< 0.005	0.36	0.01	-6.23	-40.6
15	parecis	40	39.9	4.66	0.97	1.77	0.05	12	0.09	0.04	5.5	0.21	2.78	< 0.01	< 0.005	0.05	0.01	0.02	< 0.005	0.04	0.02	0.01	-6.82	-45.8
16	parecis	80	75.3	4.54	0	3.26	0.15	26.3	0.27	0.15	10.8	0.75	3.85	0.03	< 0.005	0.2	0.03	0.01	< 0.005	< 0.005	0.04	< 0.004	-6.82	-43.7
17	parecis	32	134	6.28	21	8.88	5.19	29.5	2.42	1.27	24	0.81	2.25	0.03	< 0.005	0.03	0.01	0.01	< 0.005	< 0.005	0.01	< 0.004	-6.46	-42.0
18	parecis	10	142	6.97	88.1	0.17	0.07	0.16	16.2	8.84	0.22	< 0.1	2.71	0.03	0.01	0.02	0.01	< 0.005	< 0.005	0.01	< 0.001	< 0.004	-6.12	-39.6
19	parecis	22	32.2	5.94	10.6	0.21	0.12	4.95	0.69	0.26	2.27	4.05	8.26	0.03	0.01	0.01	0.23	0.03	< 0.005	< 0.005	0.01	0.01	-6.37	-40.8
20	Ronuro	60	8.5	5.19	1.8	0.3	0.07	0.41	0.25	0.15	0.36	< 0.1	4.34	< 0.01	< 0.005	0.02	0.02	0.01	< 0.005	< 0.005	< 0.001	< 0.004	-5.27	-33.6
21	Ronuro	120	12.8	5.02	1.32	0.23	0.04	2.42	0.11	0.03	1.25	< 0.1	3.61	< 0.01	< 0.005	0.03	0.01	0.01	< 0.005	< 0.005	0.01	< 0.004	-5.85	-38.1
22	Ronuro	100	12.4	5	1.02	0.56	0.07	2.04	0.05	0.02	1.46	< 0.1	4	< 0.01	< 0.005	0.02	0.01	0.01	< 0.005	< 0.005	< 0.001	< 0.004	-5.89	-35.8
23	Ronuro	32	7.1	5.04	0.84	0.33	0.09	0.06	0.08	0.04	0.23	< 0.1	2.8	< 0.01	< 0.005	0.03	< 0.005	0.01	< 0.005	0.01	< 0.001	0.01	-5.7	-35.8
24	Ronuro	30	5.6	5.1	0.78	0.33	0.07	0.28	0.04	0.01	0.45	< 0.1	3.28	< 0.01	< 0.005	0.02	< 0.005	< 0.005	< 0.005	< 0.005	< 0.001	< 0.004	-5.00	-29.4
25	Ronuro	8	77.1	4.58	0	4.74	0.11	23.2	0.63	1.58	0.93	9.86	1.63	< 0.01	0.01	0.13	0.03	< 0.005	< 0.005	< 0.005	0.09	< 0.004	-5.2	-31.1
26	Ronuro	100	42.8	4.58	0.7	3.57	0.16	10.6	0.33	0.13	4.2	0.53	4.04	0.01	< 0.005	0.36	0.01	0.01	< 0.005	< 0.005	0.01	< 0.004	-5.63	-33.0
27	Ronuro	38	79.5	5.82	7.75	6.2	0.66	20.3	0.06	0.02	9.93	1.36	2.5	< 0.01	< 0.005	0.02	< 0.005	0.02	< 0.005	< 0.005	< 0.001	0.01	-5.63	-33.8
28	Ronuro	45	91.8	5.07	3.89	8.87	0.15	26.6	0.06	0.01	16.3	0.19	3.11	< 0.01	< 0.005	0.03	< 0.005	0.01	< 0.005	0.02	< 0.001	< 0.004	-6.61	-36.1
29	parecis	100	16.7	5.2	2.32	0.86	0.08	3.09	0.03	0.01	3.13	< 0.1	3.96	< 0.01	< 0.005	0.02	< 0.005	< 0.005	< 0.005	< 0.005	< 0.001	< 0.004	-6.78	-37.9
30	parecis	50	5.1	5.17	1.12	0.09	0.09	0.05	0.04	0.01	0.36	< 0.1	2.96	< 0.01	< 0.005	0.02	< 0.005	0.01	< 0.005	< 0.005	< 0.001	< 0.004	-6.7	-38.5
31	parecis	152	8.2	4.77	1.24	0.43	0.08	0.09	0.06	0.01	0.89	< 0.1	2.23	< 0.01	< 0.005	0.03	< 0.005	0.01	< 0.005	0.01	< 0.001	0.01	-7.19	-41.2
32	parecis	70	6.86	4.81	1.03	0.26	0.09	0.09	0.04	0.01	0.68	< 0.1	2.14	< 0.01	< 0.005	0.02	< 0.005	0.01	< 0.005	< 0.005	< 0.001	0.01	-7.18	-41.1
33	parecis	35	5.3	5.17	1.09	0.8	0.16	2.73	0.03	0.01	1.5	0.25	2.16	< 0.01	< 0.005	0.01	< 0.005	0.01	< 0.005	< 0.005	< 0.001	< 0.004	-6.71	-41.2
34	parecis	152	18.6	5.25	0.8	2.19	0.11	2.38	0.09	0.04	2.63	0.15	4.41	0.02	< 0.005	0.04	0.01	< 0.005	< 0.005	< 0.005	< 0.001	< 0.004	-6.96	-42.2
35	parecis	60	7.9	5.6	2.7	0.25	0.08	0.63	0.07	0.29	0.38	0.87	5.94	0.03	< 0.005	0.01	0.05	0.01	< 0.005	0.02	0.02	0.01	-7.06	-43.5
36	parecis	70	21.5	6.14	10.4	0.28	0.09	0.8	0.53	0.93	0.67	2.38	8.66	0.03	0.01	0.01	0.08	0.01	< 0.005	< 0.005	0.01	< 0.004	-6.51	-44.1
37	parecis	40	122	4.59	0	18.8	0.12	13.6	0.2	0.42	0.2	20.6	3.95	0.04	< 0.005	0.95	0.09	0.15	0.01	0.01	0.21	< 0.004	-6.43	-45.3
38	parecis	30	6.4	5.2	0.74	0.2	0.09	0.13	0.05	0.01	0.28	< 0.1	2.91	0.02	< 0.005	0.02	< 0.005	0.01	< 0.005	0.01	< 0.001	0.01	-5.97	-42.3
39	parecis	48	271	4.1	0	17.3	< 0.02	88.4	4.23	1.44	25.8	4.14	3.76	0.07	0.02	1.41	0.06	0.01	0.01	0.01	0.03	0.01	-6.88	-45.4
40	parecis	60	6.51	4.88	0.63	0.09	0.08	0.12	0.05	0.01	0.24	< 0.1	2.23	< 0.01	< 0.005	0.02	< 0.005	0.01	< 0.005	< 0.005	< 0.001	< 0.004	-6.21	-39.8
41	parecis	60	8.4	4.86	1.37	0.08	0.09	0.04	0.05	0.01	0.16	< 0.1	2.7	< 0.01	< 0.005	0.02	< 0.005	0.01	< 0.005	< 0.005	< 0.001	< 0.004	-6.07	-40.6
42	parecis	96	7.1	5.33	0.96	0.39	0.10	0.42	0.06	0.03	0.46	0.13	3.83	< 0.01	< 0.005	0.02	< 0.005	0.01	< 0.005	0.01	< 0.001	0.01	-5.97	-39.6
43	parecis	100	7.2	5.46	0.65	0.03	0.07	0.11	0.05	0.01	0.13	< 0.1	3.67	< 0.01	< 0.005	0.01	< 0.005	0.01	< 0.005	0.01	< 0.001	0.01	-6.02	-40.6
44	parecis	12	37.3	6.23	14.6	3.32	0.09	0.78	2.86	1.85	1.53	< 0.1	2.08	< 0.01	0.01	< 0.005	< 0.005	0.04	< 0.005	< 0.005	0.01	< 0.004	-5.45	-37.4
45	parecis	100	397	7.79	231	3.29	6.22	< 0.04	17.9	6.7	70.2	< 0.1	10.1	2.21	0.22	0.01	0.38	0.01	< 0.005	< 0.005	0.06	< 0.004	-6.61	-42.5
46	parecis	70	118	6.45	37.1	8.01	0.13	8.28	0.09	0.02	7.52	1.72	2.67	< 0.01	< 0.005	< 0.005	< 0.005	< 0.005	< 0.005	0.01	< 0.001	< 0.004	-6.73	-43.8

Table 1. Continued...

Sample	Aquifer	Depth	Electrical conductivity	pH	HCO_3^-	Cl^-	SO_4^{2-}	NO_3^-	Ca^{2+}	Mg^{2+}	Na^+	K^+	Si	F^-	Sr^{2+}	Al^{3+}	Ba^{2+}	Fe^{2+}	Pb^{2+}	Zn^{2+}	Mn^{2+}	Cu^{2+}	$\delta^{18}O$	δ^2H
		(m)	µS/cm		mg/L																		‰	
47	parecis	40	8.9	5.39	1.85	0.71	0.09	0.82	0.08	0.02	1.86	< 0.1	2.67	< 0.01	< 0.005	0.01	< 0.005	0.01	< 0.005	< 0.005	< 0.001	< 0.004	-6.58	-40.3
48	parecis	49	5.4	4.99	0.66	0.1	0.09	0.04	0.09	0.02	0.25	< 0.1	2.52	< 0.01	< 0.005	0.01	< 0.005	0.01	< 0.005	< 0.005	< 0.001	< 0.004	-6.82	-47.4
49	parecis	80	21.7	6.48	3.79	1.06	0.09	5.29	0.12	0.02	5.18	< 0.1	2.94	< 0.01	< 0.005	0.03	< 0.005	0.04	< 0.005	0.09	< 0.001	0.01	-6.49	-44.3
50	parecis	96	8.6	4.95	0.9	0.23	0.08	0.87	0.09	0.01	0.75	< 0.1	3.47	< 0.01	< 0.005	0.03	< 0.005	0.04	< 0.005	0.01	< 0.001	< 0.004	-6.77	-45.6
51	parecis	100	7.2	4.82	0.88	0.03	0.05	0.03	0.05	0.01	0.17	< 0.1	3.5	< 0.01	< 0.005	0.16	< 0.005	0.01	< 0.005	< 0.005	< 0.001	< 0.004	-6.2	-42.1
52	parecis	95	6.6	4.94	0.99	0.05	0.10	0.06	0.05	0.01	0.16	< 0.1	3.19	< 0.01	< 0.005	0.05	< 0.005	0.04	< 0.005	< 0.005	< 0.001	< 0.004	-6.63	-44.9
53	parecis	100	2.1	5.61	3.82	0.03	0.09	0.04	0.04	0.004	0.18	< 0.1	3.48	< 0.01	< 0.005	0.01	< 0.005	0.03	< 0.005	< 0.005	< 0.001	< 0.004	-5.97	-38.3
54	parecis	75	104	4.6	0	7.45	0.08	33.8	0.74	0.28	14.1	1.02	3.83	< 0.01	0.01	0.24	0.03	0.02	< 0.005	0.01	0.02	< 0.004	-6.25	-39.2
55	parecis	72	5.9	5.29	0.78	0.09	0.09	0.58	0.06	0.01	0.3	< 0.1	3.3	< 0.01	< 0.005	0.01	< 0.005	0.03	< 0.005	< 0.005	< 0.001	0.01	-7.78	-52.0
56	parecis	75	4.2	5.11	0.66	0.03	0.06	0.15	0.06	0.01	0.14	< 0.1	3.68	< 0.01	< 0.005	0.07	< 0.005	0.03	< 0.005	0.01	< 0.001	0.01	-6.11	-39.6
57	parecis	96	229	7.12	135	1.26	0.6	2.16	17.7	4.81	21.2	3.46	22.7	0.31	0.14	0.05	0.10	0.02	< 0.005	0.02	< 0.001	< 0.004	-6.42	-43.0
58	parecis	100	173.9	7.74	370	6.53	7.67	< 0.04	48.9	20.6	50.9	1.15	12	0.16	0.81	0.01	0.36	0.03	< 0.005	< 0.005	0.05	< 0.004	-6.74	-43.9
59	Ronuro	120	10.5	5.04	1.25	0.16	0.08	1.85	0.06	0.03	1.34	< 0.1	4.21	< 0.01	< 0.005	0.01	< 0.005	0.03	< 0.005	< 0.005	< 0.001	< 0.004	-5.33	-34.0
60	Ronuro	30	13.7	5.3	1.26	0.94	0.19	2.94	0.14	0.03	2.59	0.12	3.29	< 0.01	< 0.005	0.01	< 0.005	0.03	< 0.005	< 0.005	< 0.001	< 0.004	-5.51	-32.9
61	parecis	198	234	8.4	147	0.33	0.22	0.14	4.35	1.16	52.9	< 0.1	8.04	0.09	0.16	< 0.005	0.10	< 0.005	< 0.005	< 0.005	< 0.001	< 0.004	-6.35	-39.6
62	Ronuro	30	320	5.69	7.97	28.9	0.39	92.8	1.65	0.43	47	6.08	2.8	0.07	0.01	0.07	0.02	0.01	< 0.005	0.01	0.03	< 0.004	-4.02	-22.0
63	Ronuro	40	32.5	6.19	18.5	0.13	0.12	< 0.04	2.1	1.4	0.8	1.86	13.7	0.02	0.03	< 0.005	0.03	0.03	< 0.005	0.01	< 0.001	0.01	-4.72	-26.1

Multivariate statistics

As a high number of parameters were to be evaluated, we used two distinct multivariate statistic methods to identify the set of clusters where the evaluated samples are categorized. In theory, these clusters are produced by specific chemical reactions.

Hierarchical clustering analysis

In the hierarchical cluster analysis (HCA), comparisons based on multiple parameters from different samples were made, and the samples were grouped into clusters based on their similarities or dissimilarities with each other, forming clusters step-by-step (Helstrup et al., 2007). A common alternative to performing HCA is Ward's method of merging the clusters. Ward's method uses an analysis of variance approach to evaluate the distances between clusters in order to minimize the sum of squares of any two clusters that can be formed at each step. The relative similarities between the samples were quantified using the Euclidean distance (d_{xy}) between two points x and y in p-dimensional space, which is given by Equation 1 below.

$$d_{xy} = \left[\sum_{j=1}^{p} \left(x_j - y_j \right)^2 \right] \qquad (1)$$

where j denotes each evaluated parameter.

The main advantage of cluster analysis is that it is a comparatively straightforward method to classify samples and that it presents results as a dendrogram, which is easy to interpret (Spencer, 2013). This technique permits for the evaluation of all variables, categorizing a coherent group of samples. In this study, we used PAST (Hammer et al., 2001), to performing Q-mode HCA.

Principal component analysis

The principal component analysis (PCA) technique was used to assess the interrelationship between the various water samples evaluated. PCA is a multivariate statistical procedure that makes use of an orthogonal transformation to convert a set of observations of variables, such as chemical species dissolved in water, into a set of linearly uncorrelated variable values, known as principal components. The PCA method decomposes the original matrix of original data into factor scores and factor loading matrices (Equation 2).

$$[X] = [T][P'] + [E] \qquad (2)$$

where $[X]$ denotes the standardized variable; $[T]$ corresponds to the matrix of principal components, $[P']$ means the transposition of the original data; and $[E]$ is the residual matrix.

Notably, PCA is applied to increase the participation of the variables with higher contributions while reducing those with lesser contributions. The number of main components is always less than or equal to the number of original variables. The distribution of the sample set evaluated in the PCA allows for the identification of clusters, trends, and anomalous data (outliers). In the present work, PCA was used to diagnose different trends of the components that explain greater variability in the analyzed samples. It is assumed that these different trends represent variable proportions of evapotranspiration and rock–fluid interaction and that the samples located at the ends of these trends represent the samples in which these processes are the most intense.

RESULTS

Parametric statistics and matrix of correlation

Overall, the samples have low electrical conductivities, ranging from 2.10 to 397 µS/cm in PAS and between 5.6 and 320 µS/cm in the Ronuro Aquifer. Most waters have low pHs, with values ranging from 4.0 to 8.4, and only four samples (0.06%) had a pH above 7—all from PAS. In the PAS waters, bicarbonate, nitrate, and sodium ions predominate, while in the Ronuro Aquifer, the ions with the highest concentrations are nitrate, sodium, and chloride (Table 2).

As for water quality, some samples present with nitrate, fluoride, lead, and manganese values above the limit set by the Brazilian Environmental Council (Brasil, 2008). A noticeable concentration of nitrate (> 5 mg/L) was recorded for several samples, with three samples above the acceptable value of 10 mg/L of N-NO_3^- or ~44 mg/L of NO_3^-) and two samples having values above twice the permitted limit.

Table 2. Parametric statistics of the main evaluated parameters.

	EC	**pH**	**HCO_3^-**	**Cl^-**	**SO_4^{2-}**	**NO_3^-**	**Ca^{2+}**	**Mg^{2+}**	**Na^+**	**K^+**	**Si**
	µS/cm		**mg/L**								
					Parecis Aquifer System (50 samples)						
Minimum	2.1	4.0	0.0	0.03	0.0	0.0	0.03	0.0	0.13	0.0	1.6
Maximum	397.0	8.4	370.0	23.7	8.3	88.4	48.9	20.6	70.2	20.6	22.7
Average	70.9	5.7	26.2	3.5	1.0	9.1	3.4	1.6	7.9	1.5	5.2
Std Dev	94.3	0.98	66.7	5.5	2.0	16.5	8.3	4.0	14.4	3.2	4.6
					Ronuro Aquifer (13 Samples)						
Minimum	5.6	4.6	0.0	0.13	0.04	0.0	0.04	0.01	0.23	0.0	1.6
Maximum	320.0	6.2	18.5	28.9	0.7	92.8	2.1	1.6	47.0	9.9	13.7
Average	54.9	5.2	3.6	4.3	0.2	14.1	0.4	0.3	6.7	1.5	4.1
Std Dev	85.4	0.46	5.2	7.9	0.2	25.5	0.7	0.5	13.0	3.0	3.0

In Rondônia, the Parecis Aquifer System has some areas of groundwater recharge that are quite vulnerable to surficial pollution due to the state's outcrop conditions. Moreover, practically no urban center has a sanitary sewage system, and there are large agricultural areas that cause diffuse contamination (Serviço Geológico do Brasil, 2012a). In the state of Mato Grosso, agriculture is a potential source of contamination of PAS's groundwater (through pesticides and nitrate). For the Ronuro Aquifer, even with a protected area (Parque Indígena do Xingu), which offers an apparent reduction in the contamination risk, it turns out that a large part of the springs of the tributaries of the Xingu River is outside this protected area and is subject environmental impacts (Serviço Geológico do Brasil, 2012b).

As seen in Table 3, the statistical association among the various evaluated parameters could be identified. As expected a priori, electrical conductivity is strongly correlated with the parameters HCO_3^-, Cl^-, Ca^{2+}, Mg^{2+}, and Sr^{2+}, indicating that variations in water salinity are caused by variations in this parameter.

The ion HCO_3^- is strongly correlated with Mg^{2+}, Ca^{2+}, and Sr^{2+}, suggesting that these parameters come from the same source that is possibly associated with the dissolution of carbonate cement. Although F^- can be associated with contamination by domestic sewage, it is noted that this ion has a high correlation with Sr^{2+} and a moderate one with Ca^{2+} and Mg^{2+}. It may also be associated with rock–water interaction. Additionally, the high concentration of SO_4^- may attribute sewage contamination as the source; however, its significant correlation only with F^- suggests a natural source.

In contrast, it is possible to note that the NO_3^- ion is strongly related to the Na^+ and Cl^- ions. High concentrations of these ions are indicative of domestic sewage contamination. K^+ and Ba^{2+} ions do not have a significant correlation with any other parameter, except between themselves, and cannot serve as a conclusive diagnosis for natural or anthropic processes. However, given the moderate to low correlation values (0.4-0.5) between Ba^{2+} and NO_3^-, it is possible to associate Ba^{2+} and K^+ with domestic sewage contamination.

Multivariate statistics

Hierarchical clustering of the Parecis and Ronuro aquifers

For a better understanding of the hydrochemical types, the samples were divided into three groups with the help of cluster analysis (Figure 3b). In Group 1 there are 28 samples (23 samples from PAS and five samples from the Ronuro Aquifer) that are distributed throughout the basin (Figure 3a). Most samples have electrical conductivities below 50 µS/cm (75%), with an average of 72.1 µS/cm (Figure 3c); 79% of the samples have pH values between 5 and 7 (Figure 3d). The ions with the highest concentrations are bicarbonate with an average of 43.5 mg/L and sodium with an average of 8.6 mg/L. The silica concentration with an average of 14.2 mg/L also stands out (Figure 3e). In this group, the samples are divided between sodium bicarbonates and calcium bicarbonates, with fewer sodium chlorides (Figure 4).

Group 2 consists of 20 samples (15 samples from PAS and 5 samples from the Ronuro Aquifer) that are distributed throughout the basin (Figure 3a). These samples have an average electrical conductivity of 107.1 µS/cm with the majority of the values between 50 and 150 µS/cm (65% – Figure 3c). They are more acidic samples with pH values below 7 (Figure 3d). In this group, the ions that have the highest concentrations are sodium (an average of 11.8 mg/L) and nitrate (an average of 27.5 mg/L – Figure 3e). It should be noted that two samples from this group have NO_3^- with values above the maximum allowed by CONAMA (Brasil, 2008). A large part of the samples in this group are classified as sodium chloride (80%) (Figure 4) due to higher concentrations of chloride and sodium, which are possibly associated with anthropic contamination.

In Group 3, there are 15 samples (12 samples from Parecis AS and 3 samples from the Ronuro Aquifer), all located in the state of Mato Grosso and distributed mainly in the central portion of the basin (Figure 3a). All samples have low electrical conductivities (lower than 10 µS/cm – Figure 3c) and pH values below 5.5 (Figure 3d). Even in low concentrations, silica (an

Table 3. Matrix of linear correlation (Pearson) of the main hydrochemical parameters; values above 0.80 are highlighted in bold.

	EC	**pH**	**HCO_3^-**	**F^-**	**Cl^-**	**SO_4^{2-}**	**NO_3^-**	**Ca^{2+}**	**Mg^{2+}**	**Na^+**	**K+**	**Sr^{2+}**	**Ba^{2+}**
EC													
pH	0.359												
HCO_3^-	0.777	0.639											
F^-	0.767	0.512	0.661										
Cl^-	**0.867**	0.214	0.450	0.616									
SO_4^{2-}	0.425	0.510	0.341	0.735	0.376								
NO_3^-	0.779	-0.085	0.240	0.467	**0.839**	0.253							
Ca^{2+}	**0.820**	0.626	**0.966**	0.719	0.575	0.363	0.305						
Mg^{2+}	**0.861**	0.465	**0.930**	0.710	0.592	0.290	0.409	0.922					
Na^+	0.503	0.137	0.085	0.289	0.661	0.460	0.731	0.127	0.068				
K^+	0.217	-0.031	-0.070	0.234	0.288	0.181	0.432	-0.004	0.069	0.104			
Sr^{2+}	**0.816**	0.478	0.738	**0.834**	0.688	0.451	0.446	0.786	0.868	0.131	0.145		
Ba^{2+}	0.392	0.095	0.113	0.434	0.486	0.259	0.506	0.186	0.259	0.256	0.669	0.347	

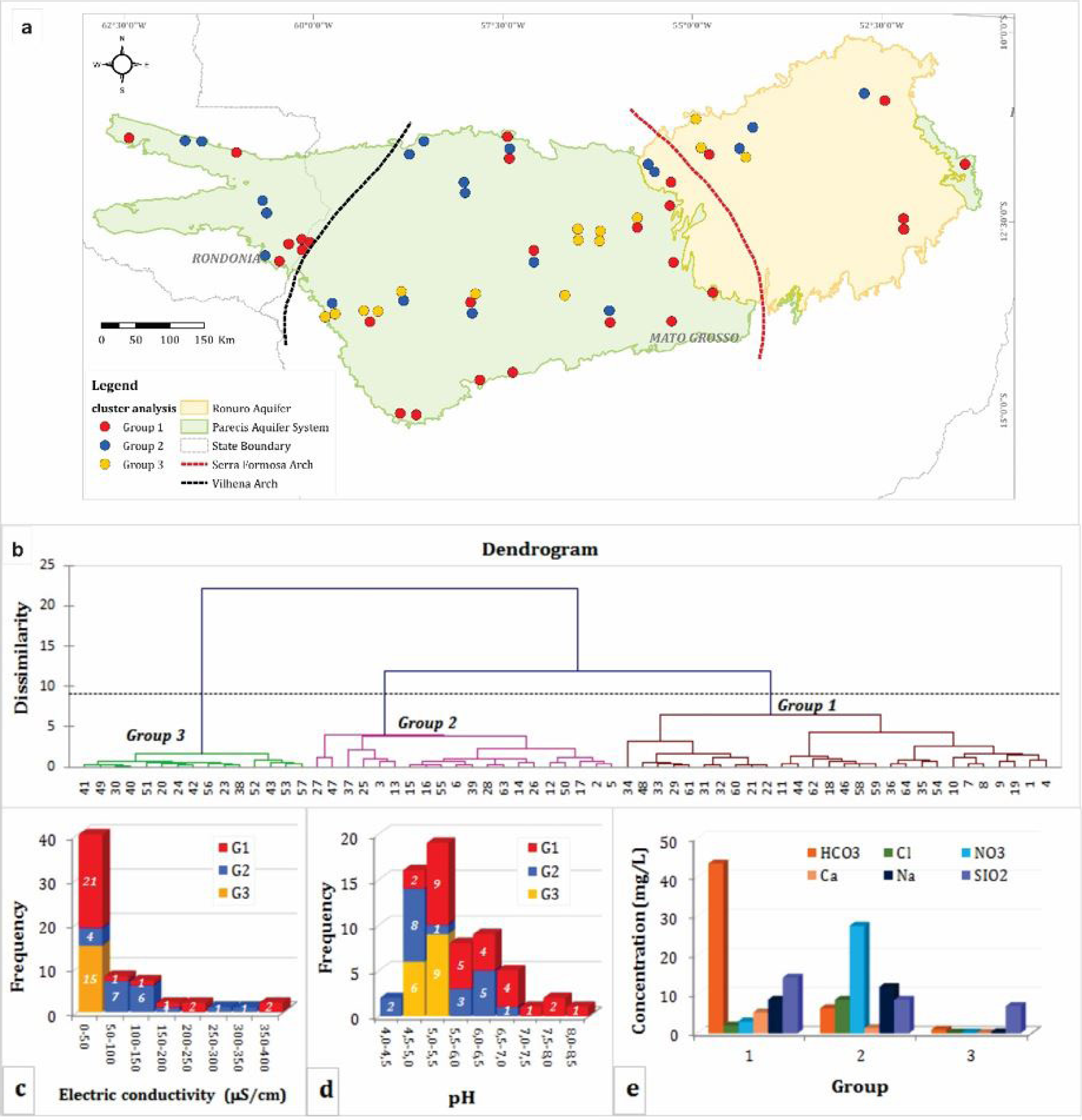

Figure 3. (a) Samples distribution map by group according to cluster analysis; (b) Dendrogram; (c) and (d) Electrical conductivity and pH histograms, respectively; (e) Averages of the major ions and silica.

average of 6.9 mg/L) and bicarbonate (an average of 0.9 mg/L – Figure 3e) stand out. The sodium bicarbonate waters predominate this group (90%), only one sample was classified as calcium bicarbonate water (Figure 4).

A Piper diagram, which is the most common approach, was used to identify the hydrochemistry of the evaluated aquifers. In the Piper diagram, there is a wide variation in the hydrochemical typology of the samples, which belong to the mixed types, sodium bicarbonate type, sodium chloride type, calcium bicarbonate type and magnesium bicarbonate type. Comparing the clustering calculated by the HCA (Figure 3a) and the hydrochemistry typology defined by the Piper diagram, showed in Figure 4, it is noted that the groups distinguished by the HCA do not correlate with the representation in the Piper diagram. Instead, the samples belonging to all groups scatter in a broad region of the diagram, indicating the distinctiveness of both methodologies.

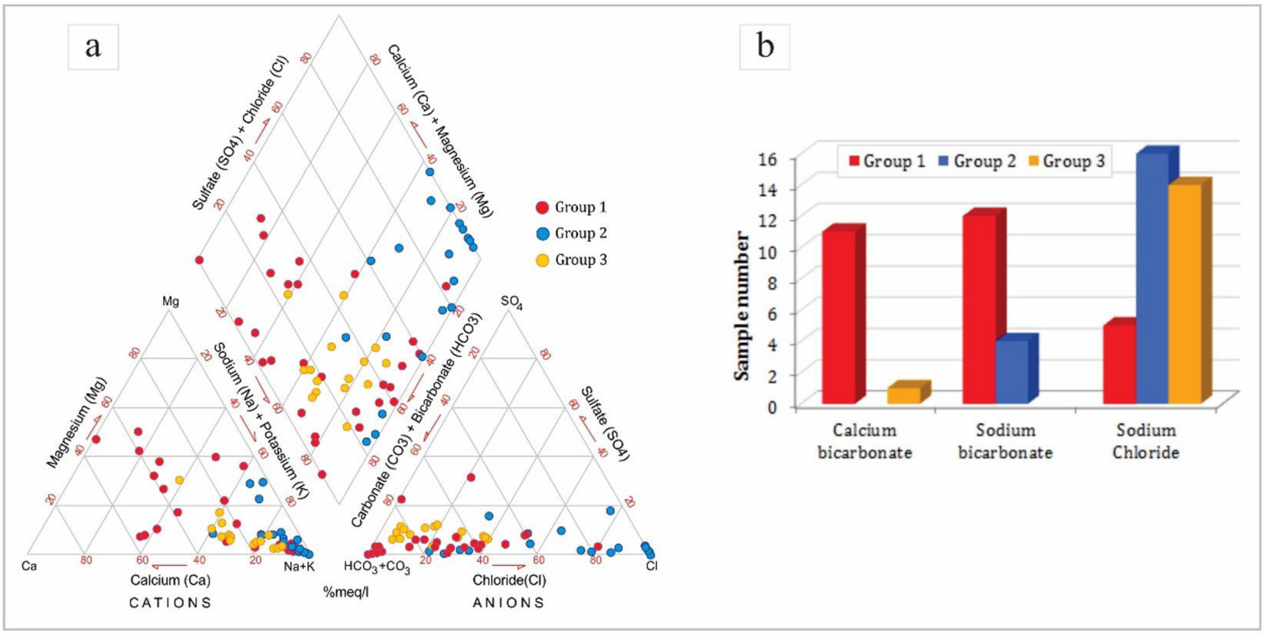

Figure 4. (a) Piper diagram; (b) Hydrochemical types of samples by groups.

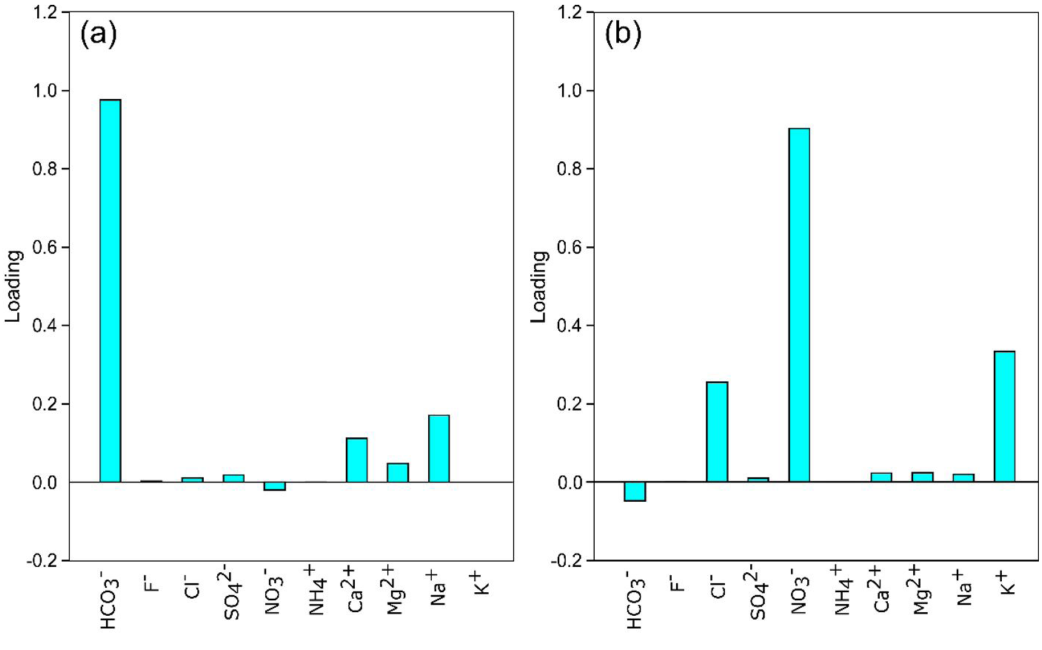

Figure 5. Loading factor to compute: (a) PCA1; (b) PCA2.

PCA of hydrochemistry data from the Parecis and Ronuro aquifers

We calculated the principal components and the factor loading of each evaluated parameter. PCA1 is related to the largest eigenvalue and explains the majority of the variance of the hydrochemistry data set, amounting to 88.1% (Figure 5). The PCA2 (orthogonal and uncorrelated with PCA1) accounts for 9.7% of the hydrochemistry variance. PCA1 is mostly determined by HCO_3^-, Ca^{2+}, Na^{2+}, and Mg^{2+} that score higher factor loadings. On the other hand, PCA2, representing 9.7% of the variance of samples, mainly determined by NO_3^-, Cl^-, and K^+.

Plotting the evaluated samples in the PCA diagram, most of the Parecis and Ronuro samples overlap in a region with low values of both PCA1 and PCA2. However, in the case of the Parecis Aquifer, some samples display high variability with respect to PCA1, while Ronuro Aquifer exhibits low variability. Both the Parecis and Ronuro Aquifers exhibit some samples and display a great variability along the PCA2 axis following a visible trend as seen in Figure 6.

Stable isotopes characterization

The $\delta^{18}O$ values of groundwater samples range from -7.8 ‰ to -4.0 ‰, while the δ2H values range from 52.0 ‰ to -22.0 ‰. Figure 5 (δ^2H vs. $\delta^{18}O$) clearly shows the meteoric origin of the sampled waters as they cluster along the Global Weather Line (Craig, 1961), as well as the local weather lines extracted using GNIP/IAEA data from Cuiabá (MT) and Porto Velho (RO) stations. The isotopic compositions differ in the two studied aquifers. As seen in Figure 7, the waters of the Ronuro Aquifer are more enriched than those of the Parecis Aquifer System. In the Ronuro Aquifer, values vary between -6.6‰ and -4.0‰ for $\delta^{18}O$ and between -38.1‰ and -22.0‰ for δ^2H, with -5.4‰ being the mean value for $\delta^{18}O$ and -32.4‰ for δ^2H. In the Parecis Aquifer System, the values are between -7.8‰ and -5.5‰ for $\delta^{18}O$ and between -52.0‰ and -37.4‰ for δ^2H, with -6.5‰ and -42.4‰ being its respective averages (Figure 7). As observed in Figure 8, the values of $\delta^{18}O$ and δ^2H follow a trend wherein it becomes more depleted with an increase in depth. However, when the depth of the wells exceeds 75 meters, this trend is not observed anymore.

DISCUSSION

The understanding of the composition of groundwater requires recognizing the possible mechanisms that can promote the release of ions into the water. We evaluated the combined use of multivariate statistics of hydrochemistry data and interpretation of the stable isotopic analysis of groundwater to discern the main process controlling the hydrochemistry of groundwater and characterize the dynamics of groundwater flux.

Initially, we investigated the key mechanisms related to controlling the hydrochemistry of Parecis and Ronuro Aquifers. Subsequently, we investigated the geological context and aquifer mineralogy to identify the rock–water interaction controlling the hydrochemistry. The filling of the Parecis Basin proceeded from the deposition of essentially siliciclastic sediments, such as conglomerates, sandstones, and shales, along with carbonate sediments in a subordinate manner (Siqueira, 1989). While the Parecis formation is mostly composed of quartz, some secondary minerals were produced during the diagenetic process, cementing the sand grains (Goldberg et al., 2011). Hematite, smectite clay, and quartz cement coatings were during the eogenetic process, while sulfates (anhydrite and barite and carbonates) were precipitated during the mesogenic process. Finally, during the telogenetic processes, the precipitation of hematite and kaolinite within secondary pores and the replacement of anhydrite by gypsum occurred.

Some ions such as HCO_3^-, Ca^{2+}, Mg^{2+}, and Sr^{2+} are positively correlated with each other (Table 3) and indisputably associated with rock–water interactions. Increases in these ions may be associated with the dissolution of carbonates, as identified by Goldberg et al. (2011). A significant correlation of the F^- ion with Ca^{2+}, Mg^{2+}, and Sr^{2+} was observed (Table 3). SO_4^{2-} does not have a significant correlation coefficient with any other parameter, except for F^-. For this reason, it is quite likely that this ion is produced by the dissolution of sulfates, whose presence was also verified by Goldberg et al. (2011). Consequently, it is possible to associate the degree of water–rock interaction with high concentrations of HCO_3^-, Ca^{2+}, Mg^{2+}, and Sr^{2+} ions and F^- and SO_4^{2-} ions. Under this assumption, the pristine groundwater ranges from low mineralized groundwater, belonging to the sodium bicarbonate type, to high mineralized groundwater belonging to the calcium bicarbonate type, reflecting the amount of dissolved carbonate. A sizeable proportion of samples were collected from urban regions, where anthropogenic contamination is expected to be high. Among the several parameters, NO_3^- is recognized as the main indicator of sewage contamination, and concentrations above evident anthropic contamination (>5 mg/L) was observed in 22 of 63 samples. The high correlation of NO_3^- with Cl^- and Na^+ reinforces the contamination mediated by human activities.

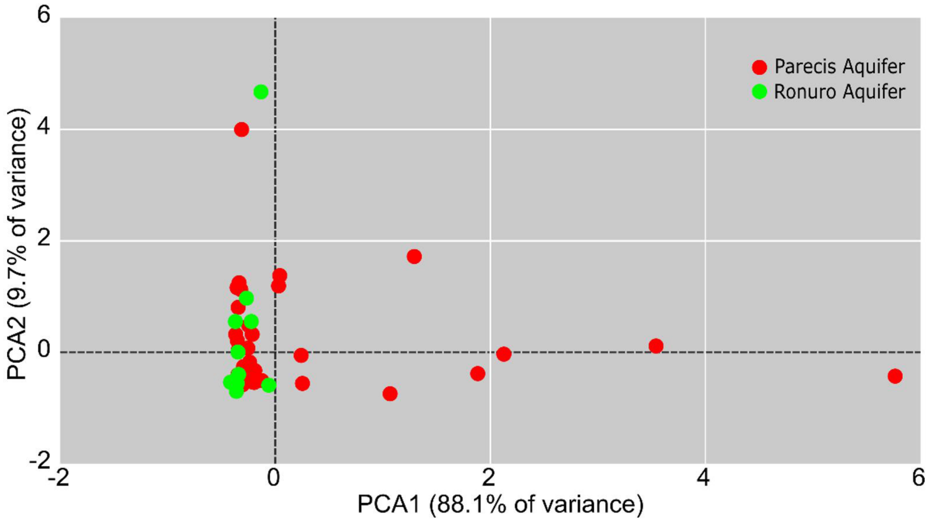

Figure 6. Groundwater samples projected in the PCA diagram (Eigenvalue scale).

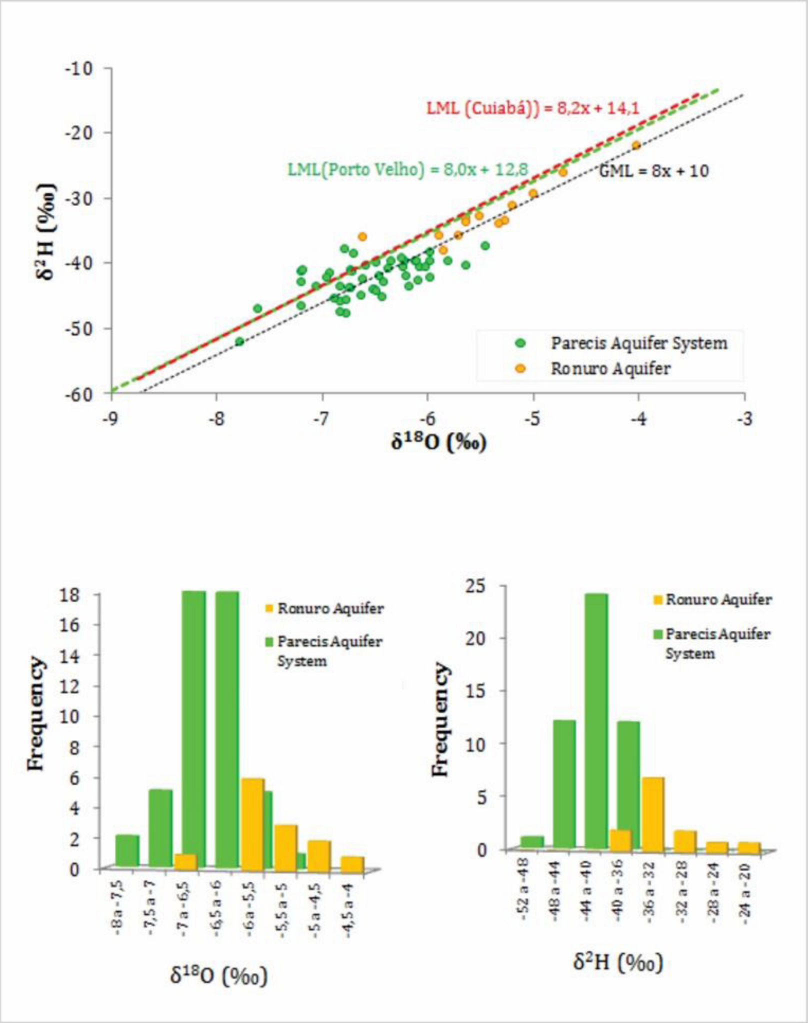

Figure 7. Plot of $\delta^{18}O$ vs. δ^2H of the samples collected with the global and local meteoric lines of Cuiabá and Porto Velho (plotted with GNIP/IAEA data) and histograms of the values of δ18O and δ^2H showing the distribution of the samples.

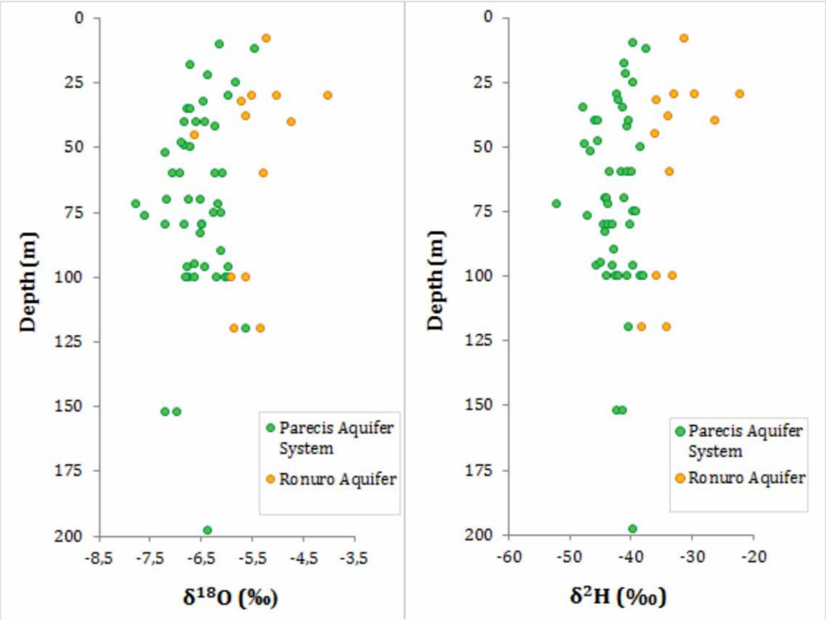

Figure 8. Values of $\delta^{18}O$ and δ^2H vs. depths of sampled wells showing a linear enrichment of both as the depth increases.

Based on the statements made above, from the coefficient of correlation analysis, we interpreted the rock–water interaction (mainly carbonate and sulfate dissolution) and sewage contamination as the main mechanisms controlling the hydrochemistry of Parecis and Ronuro Aquifers. The multivariate statics methods used here (i.e., HCA and PCA) supported this interpretation. Three distinct groups were identified in the HCA clustering samples with similar characteristics. The HCA provided a clustering dissimilar to that observed in the Piper diagram in Figure 3. The distinctiveness in the HCA and the Piper diagram is not unexpected since more parameters may be computed in the former than those used to plot the samples. Moreover, while the Piper diagram considers the proportion of some ions, the HCA considers the concentration of the evaluated ions.

The samples classified as Group 3 in the HCA are characterized by low mineralization and hydrochemistry typology—either sodium chloride or sodium bicarbonate. Likewise, Group 3 encompasses groundwater with a lower degree of interaction with the rock and reduced anthropogenic contamination. Finally, Group 2 is mostly represented by samples with a higher degree of concentration of NO_3^-, Cl^-, and Na^+ and, hence, is clearly impacted by sewage contamination.

To complement the insights provided by the HCA, we performed a PCA and verified that the position of the evaluated samples in the PCA diagram (Figure 6) does not indicate the presence of discernible clusters. We verified that most of the samples display a high variability regarding PCA1 and PCA2, with distinct trends (intermediate values) forming for both. While the largest proportion of variance is attributed to PCA1, essentially controlled by HCO_3^-, Ca^{2+} and Mg^{2+}, a minor proportion of variance is related to PCA2, which is associated with parameters such as NO_3^-, Cl^- and Na^+. Thus, the increase in PCA1 may be attributed to an increase in the level of rock–water interaction (mainly carbonate dissolution), and an increase of PCA2 may be attributed to an increase in sewage contamination. Under this interpretation, samples with low values of PCA1 and PCA2 contain pristine water derived from recent groundwater recharge. Additionality, since the Parecis Aquifer possesses superior variability with regards to PCA1, this aquifer interacted more intensively with the rock. On the other hand, Ronuro Aquifer has a low variability with respect to PCA1, indicating less interaction of groundwater with mineralogy from the host formation. This difference may be attributed to the difference in the residence time of groundwater—Ronuro Aquifer has a reduced residence time, restricting the reactions related to rock–water interaction. Based on these results, we can use the values of PCA1 to rank the status of groundwater samples in terms of rock–water interaction. On the other hand, PCA2 values may be used as a metric to quantify the level of sewage contamination. It is possible to notice that PAs and Ronuro Aquifer have the same degree of variability in relation to PC2, indicating that both have similar influences regarding the influence of contamination by domestic sewage.

From Figure 6, it is possible to note that the highest values of PCA2 can be observed in the samples with low PCA1 values, suggesting that samples displaying a high degree of interaction with groundwater are less impacted by sewage contamination. Comparing the clustering produced by the HCA, we found that Group 1 identified in the HCA is composed of samples with high PCA1 and low PCA2 values, Group 3 is composed of samples composed with low PCA1 and low PCA2 values, and Group 2 is composed of samples with low PCA1 and high PCA2 values.

The identified isotopic differences between the PAS and the Ronuro Aquifer may reflect differences in local rainfall regimes during the Holocene or may also consider climatic variations that occurred during the recharge period, and the more impoverished waters of PAS may experience more voluminous rainfall events than in the recharge areas of the Ronuro Aquifer. Interesting, as seen in Figure 7, samples from the Ronuro Aquifer are closer to the local meteoric line (LML) than samples from the Parecis Aquifer System, suggesting that groundwater from the Ronuro Aquifer are younger. This statement perfectly matches with the finding that the Ronuro Aquifer has low rock/water interaction than PAS, expressed by low variability along to PCA1 in the Principal Component Analysis diagram (Figure 6).

CONCLUSION

We made combined use of statistical analysis and isotopic characterization to understand the process controlling the water quality and infer conclusions regarding flow dynamics. From the correlation matrix used in this study, we found close associations between the major cations and anions. The highest correlation coefficient was observed among the anions HCO_3^-, Ca^{2+}, Mg^{2+}-Sr^{2+}, SO_4^{2-}, and F^- and the cations NO_3^-, Cl^-, Na^+, K^+, and Ba^{2+}. The PCA revealed that the greatest variance in the evaluated samples can be attributed to ions HCO_3^-, Ca^{2+} and Mg^{2+} related to rock–water interaction. A minor but significant proportion is related to domestic sewage contamination. While the HCA allowed the identification of three distinct groups, the PCA permitted the conclusion that the most amount of variance in the hydrochemistry of the evaluated samples is controlled by HCO_3^-, Ca^{2+}, and Mg^{2+}, which is associated with rock–water interactions. On the other hand, to a lesser degree, the variance may be also associated with NO_3^-, Cl^- and Na^+, which, in turn, is related to sewage contamination. Group 1 identified by the HCA is composed of samples with the highest level of rock–water interaction and low anthropogenic contamination, Group 3 is composed of pristine groundwater derived from a recent groundwater recharge, and Group 2 contains samples with low-level rock–water interaction and significant sewage contamination impact.

In the $\delta^{18}O$ versus δ^2H plot samples it is noted that the samples from the Ronuro Aquifer are closer to the local meteoric line than PAS, suggesting that the former is mostly derived from more recent groundwater recharge. As for the relationship between depth and isotopic values, only in shallower wells (< 75 m), it is observed that the smaller the depth, the greater the isotopic value. This change may be related to the variation of the isotopic composition of the rainwater accumulated over time, which is caused by the rainfall volume variation in Holocene.

In conclusion, this work highlights the ability of our approach of using statistical analysis of hydrochemistry to discern the main process controlling the variability of groundwater hydrochemistry, and, complementarily, the use of isotopic characterization helps identify the flow dynamics.

ACKNOWLEDGEMENTS

We gratefully acknowledge Fundação para o Desenvolvimento da UNESP – FUNDUNESP and Laboratory of Basin Studies – LEBAC/UNESP for their financial and technical support. We also thank the anonymous reviewers who pointed out important corrections to be made, which allowed us to improve our work.

REFERENCES

Agência Nacional de Águas – ANA. (2007). *Diagnóstico da outorga de direito de uso de recursos hídricos: fiscalização do uso de recursos hídricos* (Caderno de Recursos Hídricos, No. 4, 168 p.). Brasília.

Agência Nacional de Águas – ANA. (2013). *Sistemas aquíferos.* Retrieved in 2021, April 5, from http://www.metadados.inde.gov.br/

Ahada, C. P. S., & Suthar, S. (2017). Hydrochemistry of groundwater in North Rajasthan, India: chemical and multivariate analysis. *Environmental Earth Sciences*, *76*(5), 203. http://dx.doi.org/10.1007/s12665-017-6496-x.

American Public Health Association – APHA. American Water Works Association – AWWA. Water Environment Federation – WEF. (2012). *Standard methods for the examination of water and wastewater* (1368 p.). Washington.

Bahia, R. B. C. (2007). *Evolução tectonosedimentar da Bacia dos Parecis* (Tese de doutorado). Departamento de Geologia, Universidade Federal de Ouro Preto, Ouro Preto.

Bahia, R. B. C., Martins-Neto, M. A., Barbosa, M. S. C., & Pedreira, A. J. (2007). Análise da evolução tectonossedimentar da Bacia dos Parecis através de métodos potenciais. *Revista Brasileira de Geociencias*, *37*(4), 639-649. http://dx.doi.org/10.25249/0375-7536.2007374639649.

Bahia, R. B. C., Martins-Neto, M. A., Barbosa, M. S. C., & Pedreira, A. J. (2006). Revisão estratigráfica da Bacia dos Parecis - Amazonas. *Revista Brasileira de Geociencias*, *36*(4), 692-703. http://dx.doi.org/10.25249/0375-7536.2006364692703.

Barzegar, R., Asghari Moghaddam, A., Nazemi, A. H., & Adamowshi, J. (2018). Evidence for the occurrence of hydrogeochemical processes in the groundwater of Khoy plain, northwestern Iran, using ionic ratios and geochemical modeling. *Environmental Earth Sciences*, *77*(16), 597. http://dx.doi.org/10.1007/s12665-018-7782-y.

Brasil. Conselho Nacional do Meio Ambiente – CONAMA. (2008, 7 de abril). Resolução CONAMA nº 396, de 3 de abril de 2008. *Diário Oficial [da] República Federativa do Brasil*, Brasília. Retrieved in 2021, April 5, from https://www2.mma.gov.br/port/conama/legiabre.cfm?codlegi=562

Christofi, C., Bruggeman, A., Kuells, C., & Constantinou, C. (2020). Hydrochemical evolution of groundwater in gabbro of the Troodos Fractured Aquifer: a comprehensive approach. *Applied Geochemistry*, *114*, 104524. http://dx.doi.org/10.1016/j.apgeochem.2020.104524.

Craig, H. (1961). Isotopic variations in meteoric waters. *Science*, *133*(3465), 1702-1703. PMid:17814749. http://dx.doi.org/10.1126/science.133.3465.1702.

El Alfy, M., Alharbi, T., & Mansour, B. (2018). Integrating geochemical investigations and geospatial assessment to understand the evolutionary process of hydrochemistry and groundwater quality in arid areas. *Environmental Monitoring and Assessment*, *190*(5), 277. PMid:29651787. http://dx.doi.org/10.1007/s10661-018-6640-4.

Goldberg, K., Morad, S., Al-Aasm, I. S., & De Ros, L. F. (2011). Diagenesis of Paleozoic playa-lake and ephemeral-stream deposits from the Pimenta Bueno Formation, Siluro–Devonian (?) of the Parecis Basin, central Brazil. *Journal of South American Earth Sciences*, *32*(1), 58-74. http://dx.doi.org/10.1016/j.jsames.2011.05.002.

Hammer, Ø., Harper, D.A.T., & Ryan, P.D. (2001). PAST: Paleontological statistics software package for education and data analysis. *Palaeontologia Electronica*, *4*(1), 9. http://palaeo-electronica.org/2001_1/past/issue1_01.htm.

Helstrup, T., Jorgensen, N. O., & Banoeng-Yakubo, B. (2007). Investigation of hydrochemical characteristics of groundwater from the Cretaceous-Eocene limestone aquifer in southern Ghana and southern Togo using hierarchical cluster analysis. *Hydrogeology Journal*, *15*(5), 977-989. http://dx.doi.org/10.1007/s10040-007-0165-1.

International Atomic Energy Agency – IAEA. (2009) *Sampling procedures for isotope hydrology.* Retrieved in 2021, April 5, from http://www-naweb.iaea.org/napc/ih/documents/other/Sampling%20booklet%20web.pdf

Kemper, K. E. (2004). Groundwater: from development to management. *Hydrogeology Journal*, *12*(1), 3-5. http://dx.doi.org/10.1007/s10040-003-0305-1.

Kumar, P., Mahajan, A. K., & Kumar, A. (2020). Groundwater geochemical facie: implications of rock-water interaction at the Chamba city (HP), northwest Himalaya, India. *Environmental Science and Pollution Research International*, *27*(9), 9012-9026. PMid:31845247. http://dx.doi.org/10.1007/s11356-019-07078-7.

Liu, F., Wang, S., Yeh, T. C. J., Zhen, P., Wang, L., & Shi, L. (2020). Using multivariate statistical techniques and geochemical modelling to identify factors controlling the evolution of groundwater chemistry in a typical transitional area between Taihang Mountains and North China Plain. *Hydrological Processes*, *34*(8), 1888-1905. https://doi.org/10.1016/j.ecss.2020.107153.

Manoj, K., Ghosh, S., & Padhy, P. K. (2013). Characterization and classification of hydrochemistry using multivariate graphical and hydrostatistical techniques. *Research Journal of Chemical Sciences*, *3*(5), 32-34.

Marghade, D., Malpe, D. B., & Subba Rao, N. (2021). Applications of geochemical and multivariate statistical approaches for the evaluation of groundwater quality and human health risks in a semi-arid region of eastern Maharashtra, India. *Environmental Geochemistry and Health*, *43*(2), 683-703. PMid:31758364. http://dx.doi.org/10.1007/s10653-019-00478-1.

Maurya, P., Kumari, R., & Mukherjee, S. (2019). Hydrochemistry in integration with stable isotopes (δ18O and δD) to assess seawater intrusion in coastal aquifers of Kachchh district, Gujarat, India. *Journal of Geochemical Exploration*, *196*, 42-56. http://dx.doi.org/10.1016/j.gexplo.2018.09.013.

Morais, P.R.C. (1998). *Mapa Hidrogeológico do Estado de Rondônia*: texto explicativo, escala 1:1.000.000. (32p.). Porto Velho: CPRM. Programa Recursos Hídricos.

Mouser, P. J., Rizzo, D. M., Roling, W. F. M., & van Breukelen, B. M. (2005). A multivariate statistical approach to spatial representation of groundwater contamination using hydrochemistry and microbial community profiles. *Environmental Science & Technology*, *39*(19), 7551-7559. PMid:16245827. http://dx.doi.org/10.1021/es0502627.

O'Shea, B., & Jankowski, J. (2006). Detecting subtle hydrochemical anomalies with multivariate statistics: an example from 'homogeneous' groundwaters in the Great Artesian Basin, Australia. *Hydrological Processes: An International Journal*, *20*(20), 4317-4333. http://dx.doi.org/10.1002/hyp.6177.

Robins, N. S., & Fergusson, J. (2014). Groundwater scarcity and conflict–managing hotspots. *Earth Perspectives*, *1*(6), 1-9. https://doi.org/10.1186/2194-6434-1-6.

Said, I., Merz, C., Salman, S. A. E. R., Schneider, M., & Winkler, A. (2020). Identification of hydrochemical processes using multivariate statistics in a complex aquifer system of Sohag region, Egypt. *Environmental Earth Sciences*, *79*(8), 169. http://dx.doi.org/10.1007/s12665-020-08913-8.

Serviço Geológico do Brasil – CPRM. (2012a). *Relatório diagnóstico: Sistema Aquífero Parecis no Estado de Rondônia – Bacia Sedimentar dos Parecis* (Vol. 8, 40 p.). Belo Horizonte.

Serviço Geológico do Brasil – CPRM. (2012b). *Relatório diagnóstico: aquíferos Ronuro, Salto das Nuvens e Utiariti no Estado de Mato Grosso – Bacia Sedimentar dos Parecis* (Vol. 9, 55 p.). Belo Horizonte.

Silva, T. M. G. (2013). *Caracterização do sistema aquífero parecis na região centro-norte do estado de Mato Grosso: subsídios para a gestão dos recursos hídricos subterrâneos* (Dissertação de mestrado). Instituto de Geociências, Universidade de Brasília, Brasília.

Singh, K. P., Malik, A., Mohan, D., Singh, V. K., & Sinha, S. (2006). Evaluation of groundwater quality in northern Indo-Gangetic alluvium region. *Environmental Monitoring and Assessment*, *112*(1-3), 211-230. PMid:16404542. http://dx.doi.org/10.1007/s10661-006-0357-5.

Siqueira, L. P. (1989). *Bacia dos Parecis* (Boletim de Geociências da Petrobrás, No. 3, 16 p.). Rio de Janeiro.

Spencer, N. H. (2013). *Essentials of multivariate data analysis* (164 p.). Hoboken: CRC Press. http://dx.doi.org/10.1201/b16344.

Stradioto, M. R., Teramoto, E. H., & Chang, H. K. (2020a). Rock-solute reaction mass balance of water flowing within an aquifer system with geochemical stratification. *Applied Geochemistry*, *123*, 104784. http://dx.doi.org/10.1016/j.apgeochem.2020.104784.

Stradioto, M. R., Teramoto, E. H., & Chang, H. K. (2020b). Nitrato em águas subterrâneas do estado de São Paulo. *Revista do Instituto Geológico*, *40*(3), 1-12. http://dx.doi.org/10.33958/revig.v40i3.672.

Teramoto, E. H., Navarro, J., & Kiang, C. H. (2019). Avaliação geoquímica das águas envasadas de aquíferos cristalinos no sul e sudeste do Brasil. *Revista do Instituto Geológico*, *40*(2), 53-67. https://doi.org/10.33958/revig.v40i2.647.

Yang, N., Wang, G., Shi, Z., Zhao, D., Jiang, W., Guo, L., Liao, F., & Zhou, P. (2018). Application of multiple approaches to investigate the hydrochemistry evolution of groundwater in an arid region: Nomhon, Northwestern China. *Water*, *10*(11), 1667. http://dx.doi.org/10.3390/w10111667.

Authors contributions

Marcia Regina Stradioto: Conceptualization, Formal analysis, Methodology, Investigation, Writing - original draft, Writing - review & editing.

Elias Hideo Teramoto: Conceptualization, Formal analysis, Methodology, Writing - original draft, Writing - review & editing.

Hung Kiang Chang: Conceptualization, Methodology & Writing - review.

Editor-in-Chief: Adilson Pinheiro

Associated Editor: Carlos Henrique Ribeiro Lima